Article

Laser-induced Synthesis of Ultrafine Gold Nanoparticles in Covalent Organic Frameworks

ZHANG Yin and MA Shengqian✉

Received January 1, 2022
Accepted February 16, 2022

Metal nanoparticles in porous supports are of great importance for catalysis, separation and sensing, but their controllable preparation is still largely unmet. Herein, we describe a simple laser-induced synthesis of ultrafine gold nanoparticles in the covalent organic framework. Gold nanoparticles are well embedded, and they are about (1±0.1) nm in size. This work is universal for the preparation of well-dispersed and ultrafine metal nanoparticles in porous supports.

Keywords Metal nanoparticle; Covalent organic framework(COF); Ultrafine; Photoreduction

1 Introduction

Materials of superior activity and low-cost are highly desired. Metal nanoparticles in porous supports(NPPSs) belong to this category because they can reduce the cost while simultaneously maintaining the high activity of metal nanoparticles. What's more, the synergistic effect between porous supports and nanoparticles can result in novel properties. Therefore, NPPSs have been widely studied for catalysis[1,2], separation[3], and sensing[4,5], and even some of which are already being applied in industry.

In general, two strategies have been summarized for the preparation of NPPSs. This includes "bottle around ship" strategy and "ship in a bottle" strategy. In terms of the "bottle around ship" strategy, metal nanoparticles are synthesized in advance, and surround which the porous supports are prepared with the help of surfactants[6−10]. Regarding "ship in a bottle" strategy, NPPSs can be obtained by reducing metal precursors in porous supports using $NaBH_4$, solvent, or H_2[11−14]. According to the nanoscale effect, smaller nanoparticles will have higher activity, and well-dispersed ultrafine metal nanoparticles are mainly prepared *via* the "ship in a bottle" strategy[15,16]. Different porous materials have been studied as good supports for the preparation of NPPSs, such as porous silica[17], porous carbon[18], graphene[19], metal oxide[20], zeolites[21], porous organic polymers[22−25], metal-organic frameworks[15,16], organic cages[26,27], and covalent organic frameworks(COFs)[28]. Crystalline COFs have recently received much attention due to their excellent compatibility in acidic/basic environments, stability in various solvent/thermal conditions, and tunability in structure and property[29−31].

COFs typically have a pore size of about 2 nm, making them useful for the investigation of intrapore activities. Many papers have been published on the preparation of COFs-supported nanoparticles[28,32−42]. The nanoparticles are widely distributed in the range of 2—10 nm because it is difficult to control the size of nanoparticles following the "ship in a bottle" strategy with $NaBH_4$, H_2 or solvent as reducing agents[33−38]. In addition, nanoparticles tend to aggregate when they are smaller than 2 nm because of high surface free energy. Therefore, it is still challenging to prepare ultrafine nanoparticles(<2 nm) supported by COFs with a narrow size distribution. Recently, metal nanoparticles(1.5 nm) in COFs have been reported, in which COFs with phosphine/sulfur functions can stabilize metal nanoparticles *via* strong coordination[39−41]. Another study described the preparation of 1.5 nm Pd nanoparticles in COFs, in which extra —NH_2 groups introduced by the nonstoichiometric synthon strategy can effectively prevent the agglomeration of metal nanoparticles during the H_2 reduction process[42]. Herein, we realize the preparation of ultrafine (1±0.1 nm) gold nanoparticles in COFs by taking advantage of coordination between metal nanoparticles and rapid photoreduction. This operational simple and facile protocol is expected to be appliable to the preparation of other NPPSs.

2 Experimental

2.1 Preparation of TAPB-TA-COF

TAPB-TA-COF was prepared following a reported procedure[43] with slight modification. 1,3,5-Tri-(4-aminophenyl)benzene (TAPB, 0.160 mmol, 56.2 mg), terephthalaldehyde(TA, 0.24 mmol, 32.2 mg) and *o*-dichlorobenzene(*o*-DCB)/*n*-BuOH (1.0/1.0 mL) were mixed in a 5 mL Schlenk tube and sonicated to obtain a suspension. The mixture was well dispersed after the addition of acetic acid(6 mol/L, 0.2 mL). And the tube was degassed *via* three freeze-pump-thaw cycles. Keeping this reaction at 120 °C for 3 d, the yellow solid was isolated by

✉ MA Shengqian
shengqian.ma@unt.edu
Department of Chemistry, University of North Texas, Denton, TX 76201, USA

https://doi.org/10.1007/s40242-022-2002-4

centrifugation at 10000 r/min and washed with THF(6×5 mL). Soxhlet extraction with THF was used to further purify TAPB-TA-COF for 2 d. Finally, TAPB-TA-COF was obtained as a yellow powder with a yield of 80%.

2.2 Preparation of TAPB-TA-COF-Au

Typically, 1 mg of TAPB-TA-COF and 1 mL of CH_3CN were mixed in a 10 mL quartz vial, where 100 μL of $AuCl_3$ solution (1 mg/mL) was added. The vial was covered with aluminum foil to prevent light illumination and the mixture was stirred for 10 h. Then the solid was separated from the mixture by centrifugation at 10000 r/min and washed with CH_3CN(3×2 mL). The obtained solid was dispersed in the 10 mL quartz vial with 1 mL of CH_3CN and the suspension was irradiated by a 523 nm laser for 10 min under vigorous stirring. Then the vial was covered with aluminum foil again and the obtained solution is ready for further use. The Au content is 3.5% as determined by inductive coupled plasma emission spectrometry(ICP).

2.3 Reagents

All the chemicals were purchased from commercial resources and used without further purification unless otherwise stated. Corresponding information of representative chemicals was given below: terephthalaldehyde(Sigma, 99.5%), 1,2-dichlorobenzene(Alfa, 99.5%), 1-butanol(Alfa, 99.5%), tetrahydrofuran(Sigma, 99.5%), gold trichloride(Alfa, 99.9%), and acetonitrile(Sigma, 99.8%), and 1,3,5-tri-(4-aminophenyl) benzene was synthesized according to the literature[44].

2.4 Characterization

Fourier transform infrared(FTIR) spectra were recorded on a Spectrum One(Perkin Elmer Instruments Co., Ltd.) with KBr as the background in the spectral range of 400—4000 cm^{-1}. Wide-angle powder X-ray diffraction(XRD) patterns were obtained at a scanning rate of 4°/min using D/MAX-TTRIII (CBO)(Rigaku Corporation) with Cu $K\alpha$ radiation(λ=0.154 nm) operating at 200 kV and 40 mA. X-Ray photoelectron spectroscopy(XPS) spectra were achieved by an ESCALAB 20 Xi XPS system, where the analysis chamber was 1.5×10^{-9} mbar (1.5×10^{-7} Pa) and the size of X-ray spot was 500 μm. Brunauer-Emmett and Teller(BET) surface areas were determined using an ASAP2420-4(Micromeritics Instrument Corporation) surface analyzer at 77 K, and before measurement, the samples were activated at 120 °C for 12 h under vacuum. Transmission electron microscopy(TEM) images were performed on a Tecnai G2 F20 S-TWIN with an acceleration voltage of 200 kV.

3 Results and Discussion

A COF with a pore size of about 3 nm was chosen as the representative platform. Specifically, Scheme 1 describes the entire experimental procedure.

COF is prepared from 1,3,5-tris-(4-aninophenyl) benzene (TAPB) and TA. The characteristic peaks agree well with the literature[43] data on the obtained patterns of powder X-ray diffraction(PXRD)(Fig.1), confirming the successful

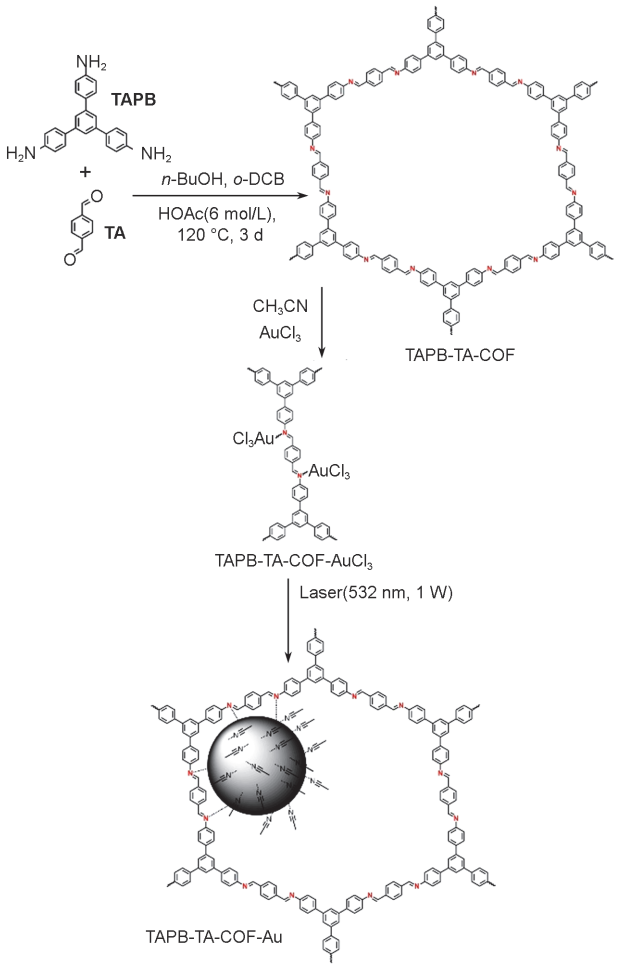

Scheme 1 Preparation of TAPB-TA-COF-Au

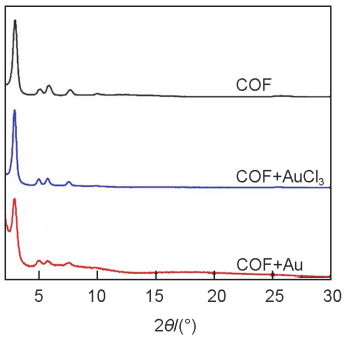

Fig.1 PXRD patterns of TAPB-TA-COF, TAPB-TA-COF-$AuCl_3$ and TAPB-TA-COF-Au

https://doi.org/10.1007/s40242-022-2002-4

preparation of crystalline TAPB-TA-COF. Purified TAPB-TA-COF is in yellow color when dispersed in CH_3CN and turns brown rapidly after the addition of $AuCl_3$ solution(1 mg/mL) [Fig.2(A)]. The color change is caused by the coordination between the —C═N— and the $AuCl_3$. As seen in the Fourier transform infrared(FTIR) spectra[Fig.2(B)], the shifting peak at 1603 cm^{-1} and the new peak at 1654 cm^{-1} compared to the original —C═N— stretching vibration at 1593 and 1620 cm^{-1} are attributed to the coordination[28]. In addition, X-ray photoelectron spectroscopy(XPS) shows the change of N_{1s} from 398.61 eV to 399.36 eV[Fig.2(C)] after the addition of $AuCl_3$ solution to the TAPB-TA-COF suspension, which is another evidence for the interaction between the —C═N— and $AuCl_3$[28]. Meanwhile, the resulted TAPB-TA-COF-$AuCl_3$ has the same crystallinity as TAPB-TA-COF(Fig.1), indicating that the interaction between TAPB-TA-COF and $AuCl_3$ does not destroy the structure. The obtained TAPB-TA-COF-$AuCl_3$ is redispersed in CH_3CN and illuminated with a 532 nm laser (1 W) for 10 min under vigorous stirring, leading to the TAPB-TA-COF-$AuCl_3$ to TAPB-TA-COF-Au transformation. Au_{4f} XPS double peaks[Fig.2(D)] show the reduction of $AuCl_3$ to Au nanoparticles with a 0.8 eV difference between TAPB-TA-COF-$AuCl_3$(84.31 eV, 87.91 eV) and TAPB-TA-COF-Au(85.11 eV, 88.71 eV).

The presence of metal nanoparticles can be imaged by transmission electron microscopy(TEM). Au nanoparticles are absent in both TAPB-TA-COF and TAPB-TA-COF-$AuCl_3$ [Fig.3(A) and (B)], while they are obviously observed in Fig.3(C) with the size of (1±0.1) nm. Both size diameter and size distribution of nanoparticles are comparable to those reported works[39—42], and the rapid photoreduction is advantageous for generating small nanoparticles with the intrinsic pore environment(—C═N—) and the solvent(CH_3CN) serving as stabilizing agents.

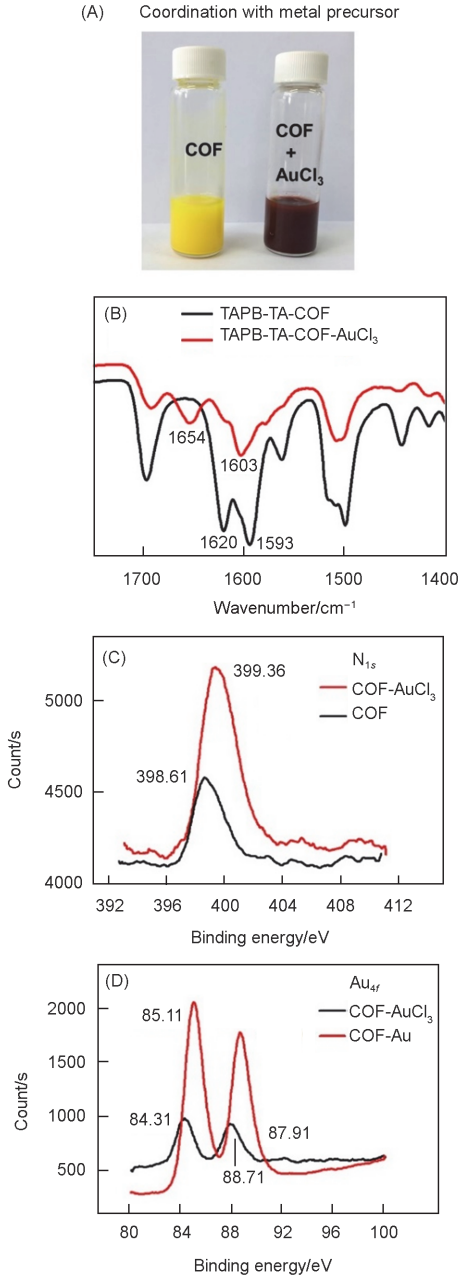

Fig.2 Photos for the COF suspension before and after the addition of $AuCl_3$(A), FTIR spectra of TAPB-TA-COF and TAPB-TA-COF-$AuCl_3$(B), XPS spectra of TAPB-TA-COF, TAPB-TA-COF-$AuCl_3$ and TAPB-TA-COF-Au(C and D)

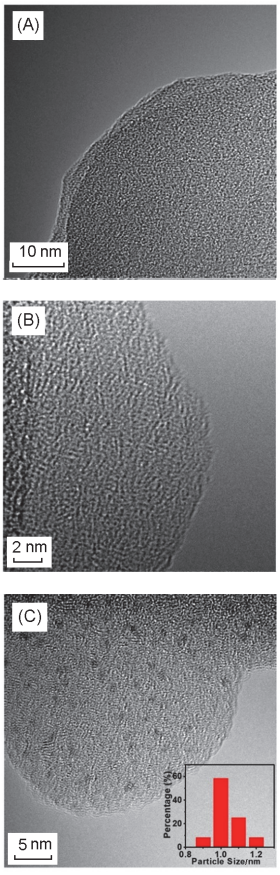

Fig.3 TEM images of TAPB-TA-COF(A), TAPB-TA-COF-$AuCl_3$(B) and TAPB-TA-COF-Au(C) with the inset in (C) being the size distribution of Au nanoparticles

https://doi.org/10.1007/s40242-022-2002-4

In addition, TAPB-TA-COF-Au retains the original structure of TAPB-TA-COF(Fig.1). The stability of the gold nanoparticles is good, which is proposed to be favored by the interaction with —C═N— of COF and coordination with CH_3CN(Scheme 1). Another key factor in NPPSs is maintaining the porosity and the surface areas of the support. According to the N_2 sorption isotherms of both TAPB-TA-COF and TAPB-TA-COF-Au[Fig.4(A)], the respective Brunauer-Emmett and Teller(BET) surface areas are 1521 and 1023 m^2/g, confirming good surface areas. The pore size distribution curves for TAPB-TA-COF and TAPB-TA-COF-Au[Fig.4(B)] show that the major pore size is 3 nm, indicating the good maintenance of porosity.

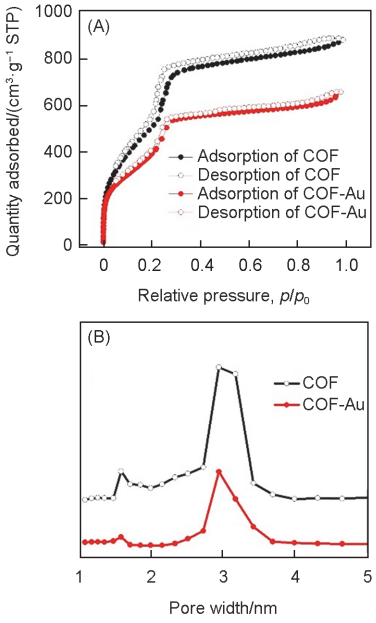

Fig.4 N_2 sorption isotherms(A) and pore size distribution(B) of the as-prepared TAPB-TA-COF and TAPB-TA-COF-Au

4 Conclusions

In summary, it should be noted that TAPB-TA-COF-Au was prepared using an operationally simple and facile photoreduction strategy. The resulting gold nanoparticles [(1±0.1) nm] were stable and well dispersed in TAPB-TA-COF. This work will be a necessary reference for the preparation of NPPSs.

Acknowledgements

This work was supported by the Robert A. Welch Foundation(No.B-0027).

Conflicts of Interest

The authors declare no conflicts of interest.

References

[1] Guo F., Yang H., Aguila B., Al-Enizi A., Nafady A., Singh M., Bansal V., Ma S., *Catal. Sci. Technol.*, **2018**, *8*, 5244

[2] Sun Q., Chen M., Aguila B., Nguyen N., Ma S., *Faraday Discuss*, **2017**, *201*, 317

[3] Khorsandkheirabad A., Zhou X., Xie D., Wang H., Yuan J., *Macromol. Rapid Comm.*, **2021**, *42*, 2000143

[4] Li Z., Qiao X., He G., Sun X., Feng D., Hu L., Xu H., Xu H., Ma S., Tian J., *Nano Res.*, **2020**, *13*, 3377

[5] Wang Y., Wang L., Chen H., Hu X., Ma S., *ACS Appl. Mater. Interfaces*, **2016**, *8*, 18173

[6] Lu G., Li S., Guo Z., Farha O., Hauser B., Qi X., Wang Y., Wang X., Han S., Liu X., DuChene J., Zhang H., Zhang Q., Chen X., Ma J., Loo S., Wei W., Yang Y., Hupp J., Huo F., *Nat. Chem.*, **2012**, *4*, 310

[7] Guo Z., Xiao C., Maligal-Ganesh R., Zhou L., Goh T., Lin X., Tesfagaber D., Thiel A., Huang W., *ACS Catal.*, **2014**, *4*, 1340

[8] Kuo C., Tang Y., Chou L., Sneed B., Brodsky C., Zhao Z., Tsung C., *J. Am. Chem. Soc.*, **2012**, *134*, 14345

[9] Zhang Z., Chen Y., Xu X., Zhang J., Xiang G., He W., Wang X., *Angew. Chem. Int. Ed.*, **2013**, *53*, 429

[10] Zhao Y., Kornienko N., Liu Z., Zhu C., Asahina S., Kuo T., Bao W., Hexemer A., Terasaki O., Yang P., Yaghi O., *J. Am. Chem. Soc.*, **2015**, *137*, 2199

[11] Hwang Y., Hong D., Chang J., Jhung S., Seo Y., Kim J., Vimont A., Daturi M., Serre C., Férey G., *Angew. Chem. Int. Ed.*, **2008**, *120*, 4212

[12] Aijaz A., Akita T., Tsumori N., Xu Q., *J. Am. Chem. Soc.*, **2013**, *135*, 16356

[13] Aijaz A., Karkamkar A., Choi Y., Tsumori N., Rönnebro E., Autrey T., Shioyama H., Xu Q., *J. Am. Chem. Soc.*, **2012**, *134*, 13926

[14] Guo J., Duan Y., Liu Y., Li X., Zhang Y., Long C., Wang Z., Yang Y., Zhao S., *J. Mater. Chem. A*, **2022**, Doi:10.1039/D1TA08319H

[15] Yang Q., Xu Q., Jiang H., *Chem. Soc. Rev.*, **2017**, *46*, 4774

[16] Li G., Zhao S., Zhang Y., Tang Z., *Adv. Mater.*, **2018**, *30*, 1800702

[17] Shang L., Bian T., Zhang B., Zhang D., Wu L., Tung C., Yin Y., Zhang T., *Angew. Chem. Int. Ed.*, **2014**, *53*, 250

[18] Joo S., Choi S., Oh L., Kwak J., Liu Z., Terasaki O., Ryoo R., *Nature*, **2001**, *412*, 169

[19] Nethravathi C., Anumol E., Rajamathi M., Ravishankar N., *Nanoscale*, **2011**, *3*, 569

[20] Wang W., An W., Ramalingam B., Mukherjee S., Niedzwiedzki D., Ganggopadhyay S., Biswas P., *J. Am. Chem. Soc.*, **2012**, *134*, 11276

[21] Farrusseng D., Tuel A., *New J. Chem.*, **2016**, *40*, 3933

[22] Gong W., Wu Q., Jiang G., Li G., *J. Mater. Chem. A*, **2019**, *7*, 13449

[23] Cui C., Tang Y., Ziaee M., Tian D., Wang R., *ChemCatChem*, **2018**, *10*, 1431

[24] Khatletskaya K., Reboul J., Meilikhov M., Nakahama M., Diring S., Tsujimoto M., Isoda S., Kim F., Kamei K., Fischer R., Kitagawa S., Furukawa S., *J. Am. Chem. Soc.*, **2013**, *135*, 10998

[25] Cao H., Huang H., Chen Z., Karadeniz B., Lü J., Cao R., *ACS Appl. Mater. Interfaces*, **2017**, *9*, 5231

[26] Sun N., Wang C., Wang H., Yang L., Jin P., Zhang W., Jiang J., *Angew. Chem. Int. Ed.*, **2019**, *58*, 18011

[27] Yang X., Sun J., Kitta M., Pang H., Xu Q., *Nat. Catal.*, **2018**, *1*, 214

[28] Ding S., Gao J., Wang Q., Zhang Y., Song W., Wang W., *J. Am. Chem. Soc.*, **2011**, *133*, 19816

[29] Song Y., Sun Q., Aguila B., Ma S., *Adv. Sci.*, **2019**, *6*, 1801410

[30] Diercks C., Yaghi O., *Science*, **2017**, *355*, eaal1585

[31] Geng K., He T., Liu R., Dalapati S., Tan K., Li Z., Tao S., Gong Y., Jiang Q., Jiang D., *Chem. Rev.*, **2020**, *120*, 8814

[32] Zhang C., Cui M., Ren J., Xing Y., Zhao H., Liu P., Ji X., Li M., *Chem. Eng. J.*, **2020**, *401*, 126025

[33] Lan X., Du C., Cao L., She T., Li Y., Bai G., *ACS Appl. Mater. Interfaces*, **2018**, *10*, 38953

[34] Fan M., Wang W., Wang X., Zhu Y., Dong Z., *Ind. Eng. Chem. Res.*, **2020**, *59*, 12677

[35] Jin P., Niu X., Gao Z., Xue X., Zhang F., Cheng W., Ren C., Du H., Manyande A., Chen H., *ACS Appl. Nano Mater.*, **2021**, *4*, 5834

[36] Chen G., Li X., Zhao C., Ma H., Kan J., Xin Y., Chen C., Dong Y., *Inorg. Chem.*, **2018**, *57*, 2678

[37] Wang N., Liu J., Tang L., Wei X., Wang C., Li X., Ma L., *ACS Appl. Mater. Interfaces*, **2021**, *13*, 24966

[38] Zhai L., Yang S., Yang X., Ye W., Wang J., Chen W., Guo Y., Mi L., Wu Z., Soutis C., Xu Q., Jiang Z., *Chem. Mater.*, **2020**, *32*, 9747

[39] Lu S., Hu Y., Wan S., McCaffrey R., Jin Y., Gu H., Zhang W., *J. Am. Chem. Soc.*, **2017**, *139*, 17082

[40] Deng Y., Zhang Z., Du P., Ning X., Wang Y., Zhang D., Liu J., Zhang S., Lu X., *Angew. Chem. Int. Ed.*, **2020**, *59*, 6082

[41] Tao R., Shen X., Hu Y., Kang K., Zheng Y., Luo S., Yang S., Li W., Lu S., Jin Y., Qiu L., Zhang W., *Small*, **2020**, *16*, 1906005

[42] Xu C., Lin J., Yan D., Guo Z., Austin D., Zhan H., Kent A., Yue Y., *ACS Appl. Nano Mater.*, **2020**, *3*, 6416

[43] Xu H., Gao J., Jiang D., *Nat. Chem.*, **2015**, *7*, 905

[44] Sun Q., Aguila B., Perman J., Earl L., Abney C., Cheng Y., Wei H., Nguyen N., Wojtas L., Ma S., *J. Am. Chem. Soc.*, **2017**, *139*, 2786